

Figure 7.13 Chart illustrating transformation relationships among the forms of gallium oxide and its hydrates. Conversion (wet) of the phase designated as $\text{Ga}_{2-x}\text{Al}_x\text{O}_3$ to $\beta\text{-Ga}_2\text{O}_3$ occurs only where $x < 1.3$; where $x > 1.3$ an $\alpha\text{-Al}_2\text{O}_3$ structure forms.

of the hydrated oxide $\text{Tl}_2\text{O}_3 \cdot 1\frac{1}{2}\text{H}_2\text{O}$ and desiccation; single crystals have a very low electrical resistivity (e.g. 7×10^{-5} ohm cm at room temperature). A mixed oxide Tl_4O_3 (black) is known and also a violet peroxide $\text{Tl}^{\text{I}}\text{O}_2$ made by electrolysis of an aqueous solution of Tl_2SO_4 and oxalic acid between Pt electrodes. TlOH has been mentioned previously (p. 226).

7.3.4 Ternary and more complex oxide phases

This section considers a number of extremely important structure types in which Al combines with one or more other metals to form a mixed oxide phase. The most significant of these from both a theoretical and an industrial viewpoint are spinel (MgAl_2O_4) and related compounds, Na- β -alumina ($\text{NaAl}_{11}\text{O}_{17}$) and related phases, and tricalcium aluminate ($\text{Ca}_3\text{Al}_2\text{O}_6$) which is a major constituent of Portland cement. Each of these compounds raises points of fundamental importance in solid-state chemistry and each possesses properties of crucial significance to

modern technology. For aluminosilicates see p. 351 and for aluminophosphates see p. 526.

Spinel and related compounds⁽⁵⁶⁾

Spinel form a large class of compounds whose crystal structure is related to that of the mineral spinel itself, MgAl_2O_4 . The general formula is AB_2X_4 and the unit cell contains 32 oxygen atoms in almost perfect ccp array, i.e. $\text{A}_8\text{B}_{16}\text{O}_{32}$. In the normal spinel structure (Fig. 7.14) 8 metal atoms (A) occupy tetrahedral sites and 16 metal atoms (B) occupy octahedral sites, and the structure can be regarded as being built up of alternating cubelets of ZnS-type and NaCl-type structures. The two factors that determine which combinations of atoms can form a spinel-type structure are (a) the total formal cation charge, and (b) the relative sizes of the 2 cations with respect both to each other and to the

⁵⁶ N. N. GREENWOOD, *Ionic Crystals, Lattice Defects and Nonstoichiometry*, Butterworths, London, 1968, 194 pp. See also J. K. BURDETT, G. D. PRICE and S. L. PRICE, *J. Am. Chem. Soc.* **104**, 92-5 (1982).

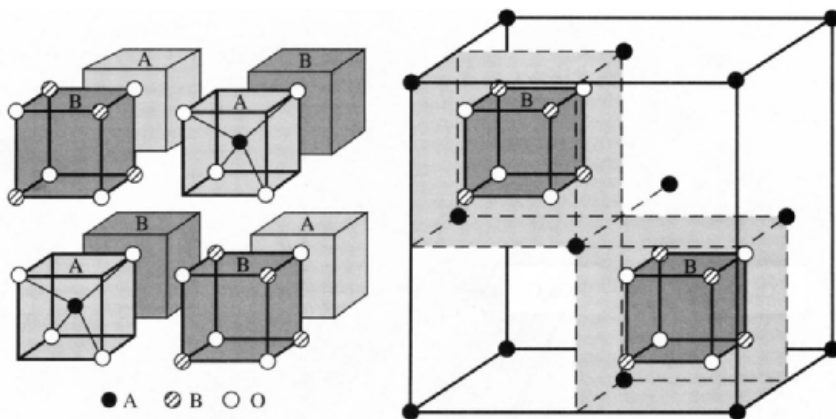
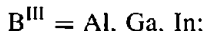
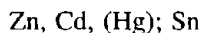


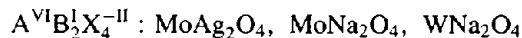
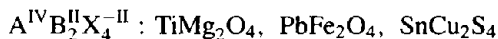
Figure 7.14 Spinel structure AB₂O₄. The structure can be thought of as 8 octants of alternating AO₄ tetrahedra and B₄O₄ cubes as shown in the left-hand diagram; the 4O have the same orientation in all 8 octants and so build up into a fcc lattice of 32 ions which coordinate A tetrahedrally and B octahedrally. The 4 A octants contain 4 A ions and the 4 B octants contain 16 B ions. The unit cell is completed by an encompassing fcc of A ions (●) as shown in the right-hand diagram; this is shared with adjacent unit cells and comprises the remaining 4 A ions in the complete unit cell A₈B₁₆O₃₂. The location of two of the B₄O₄ cubes is shown for orientation.

anion. For oxides of formula AB₂O₄ charge balance can be achieved by three combinations of cation oxidation state: A^{II}B^{III}₂O₄, A^{IV}B^{II}₂O₄, and A^{VI}B^I₂O₄. The first combination is the most numerous and examples are known with



The anion can be O, S, Se or Te. Most of the A^{II} cations have radii (6-coordinate) in the range 65–95 pm and larger cations such as Ca^{II} (100 pm) and Hg^{II} (102 pm) do not form oxide spinels. The radii of B^{III} fall predominantly in the range 60–70 pm though Al^{III} (53 pm) is smaller, and In^{III} (80 pm) normally forms sulfide spinels only.

Examples of spinels with other combinations of oxidation state are:



Many of the spinel-type compounds mentioned above do not have the normal structure in which A are in tetrahedral sites (t) and B are in octahedral sites (o); instead they adopt the inverse spinel structure in which half the B cations occupy the tetrahedral sites whilst the other half of the B cations and all the A cations are distributed on the octahedral sites, i.e. (B)_t[AB]_oO₄. The occupancy of the octahedral sites may be random or ordered. Several factors influence whether a given spinel will adopt the normal or inverse structure, including (a) the relative sizes of A and B, (b) the Madelung constants for the normal and inverse structures, (c) ligand-field stabilization energies (p. 1131) of cations on tetrahedral and octahedral sites, and (d) polarization or covalency effects.⁽⁵⁶⁾

Thus, if size alone were important it might be expected that the smaller cation would occupy the site of lower coordination number, i.e. A_t[MgAl]_oO₄; however, in spinel itself this is outweighed by the greater lattice energy achieved by having the cation of higher charge, (Al^{III}) on the site of higher coordination and

the normal structure is adopted: $(\text{Mg})_t[\text{Al}_2]_o\text{O}_4$. An additional factor must be considered in a spinel such as NiAl_2O_4 since the crystal field stabilization energy of Ni^{II} is greater in octahedral than tetrahedral coordination; this redresses the balance, making the normal and inverse structures almost equal in energy and there is almost complete randomization of all the cations on all the available sites: $(\text{Al}_{0.75}\text{Ni}_{0.25})_t[\text{Ni}_{0.75}\text{Al}_{1.25}]_o\text{O}_4$.

Inverse and disordered spinels are said to have a defect structure because all crystallographically identical sites within the unit cell are not occupied by the same cation. A related type of defect structure occurs in valency disordered spinels where, for example, the divalent A^{II} cations in AB_2O_4 are replaced by equal numbers of M^{I} and M^{III} of appropriate size. Thus, in spinel itself, which can be written $\text{Mg}_8\text{Al}_{16}\text{O}_{32}$, the 8Mg^{II} (72 pm) can be replaced by 4Li^{I} (76 pm) and 4Al^{III} (53 pm) to give $\text{Li}_4\text{-Al}_{20}\text{O}_{32}$, i.e. LiAl_5O_8 . This has a defect spinel structure in which two-fifths of the Al occupy all the tetrahedral sites: $(\text{Al}_2^{\text{III}})_t[\text{Li}^{\text{I}}\text{Al}_3^{\text{III}}]_o\text{O}_8$. Other compounds having this cation-disordered spinel structure are LiGa_5O_8 and LiFe_5O_8 . Disordering on the tetrahedral sites occurs in CuAl_5S_8 , CuIn_5S_8 , AgAl_5S_8 and AgIn_5S_8 , i.e. $(\text{Cu}^{\text{I}}\text{Al}^{\text{III}})_t[\text{Al}_4^{\text{III}}]_o\text{S}_8$, etc. Valency disordering can also be achieved by replacing A^{II} completely by M^{I} , thus necessitating replacement of half the B^{III} by M^{IV} , e.g. $(\text{Li}^{\text{I}})_t[\text{Al}^{\text{III}}\text{Ti}^{\text{IV}}]_o\text{O}_4$. Even more extensive substitution of cations has been achieved in many cubic spinel phases, e.g. $\text{Li}_5\text{Zn}^{\text{II}}\text{Al}_5^{\text{III}}\text{Ge}_9^{\text{IV}}\text{O}_{36}$ (and the Ga^{III} and Fe^{III} analogues), and the possibilities are virtually limitless.

The sensitive dependence of the electrical and magnetic properties of spinel-type compounds on composition, temperature, and detailed cation arrangement has proved a powerful incentive for the extensive study of these compounds in connection with the solid-state electronics industry. Perhaps the best-known examples are the ferrites, including the extraordinary compound magnetite Fe_3O_4 (p. 1080) which has an inverse spinel structure $(\text{Fe}^{\text{III}})_t[\text{Fe}^{\text{II}}\text{Fe}^{\text{III}}]_o\text{O}_4$.

It will also be recalled that $\gamma\text{-Al}_2\text{O}_3$ (p. 243) has a defect spinel structure in which not all of the cation sites are occupied, i.e. $\text{Al}_{21\frac{1}{3}}^{\text{III}}\square_{2\frac{2}{3}}\text{O}_{32}$: the relation to spinel $(\text{Mg}_8^{\text{II}}\text{Al}_{16}^{\text{III}}\text{O}_{32})$ is obvious, the 8Mg^{II} having been replaced by the isoelectronically equivalent $5\frac{1}{3}\text{Al}^{\text{III}}$. This explains why MgAl_2O_4 can form a complete range of solid solutions with $\gamma\text{-Al}_2\text{O}_3$: the oxygen builds on to the complete fcc oxide ion lattice and the Al^{III} gradually replaces Mg^{II} , electrical neutrality being achieved simply by leaving 1 cation site vacant for each 3Mg^{II} replaced by 2Al^{III} .

Sodium- β -alumina and related phases⁽⁵⁷⁾

Sodium- β -alumina has assumed tremendous importance as a solid-state electrolyte since its very high electrical conductivity was discovered at the Ford Motor Company by J. T. Kummer and N. Weber in 1967. The compound, which has the idealized formula $\text{NaAl}_{11}\text{O}_{17}(\text{Na}_2\text{O}\cdot 11\text{Al}_2\text{O}_3)$ was originally thought to be a form of Al_2O_3 and hence called β -alumina (1916); the presence of Na, which was at first either undetected or ignored, is now known to be essential for stability. X-ray analysis shows that the structure is closely related to that of spinel, no fewer than 50 of the 58 atoms in the unit cell being arranged exactly as in spinel. The large Na atoms are situated exclusively in loosely packed planes together with an equal number of O atoms as shown in Fig. 7.15; these planes are 1123 pm apart, being separated by the "spinel blocks". The close-packed oxygen layers above and below the Na planes are mirror images of each other 476 pm apart and they are bound together not only by the Na atoms but by an equal number of Al-O-Al bonds. There are several other sites in the mirror plane which can physically accommodate Na and this permits rapid two-dimensional diffusion of Na within the basal

⁵⁷ J. T. KUMMER, *Prog. Solid State Chem.* **7**, 141–75 (1972).
J. H. KENNEDY, *Topics in Applied Physics* **21**, 105–41 (1977).

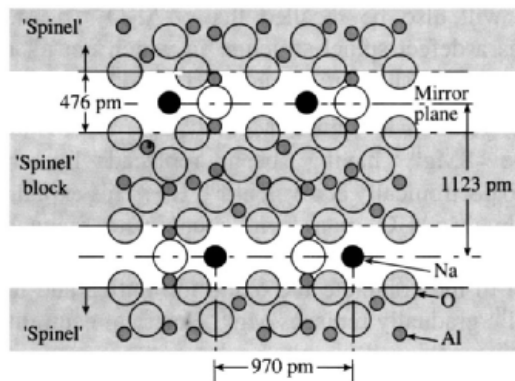


Figure 7.15 Crystal structure of Na- β -alumina (see text). This section, which is a plane parallel to the c -axis, does not show the closest Na–Na distance.

plane; it also explains the very low resistivity of the order of 30 ohm cm. The structure can also accommodate supernumerary Na ions, and the compound, even in the form of single crystals, is massively defective, having typically 20–30% more Na than indicated by the idealized formula; this is probably compensated by additional Al vacancies in the “spinel blocks” adjacent to the mirror planes, e.g. $\text{Na}_{2.58}\text{Al}_{21.8}\text{O}_{34}$.

Sodium- β -alumina can be prepared by heating Na_2CO_3 (or NaNO_3 or NaOH) with any modification of Al_2O_3 or its hydrates to $\sim 1500^\circ$ in a Pt vessel suitably sealed to avoid loss of Na_2O (as $\text{Na} + \text{O}_2$). In the presence of NaF or AlF_3 a temperature of 1000° suffices. Na- β -alumina melts at $\sim 2000^\circ$ (probably incongruently) and has d 3.25 g cm $^{-3}$. The Na can be replaced by Li, K, Rb, Cu^{I} , Ag^{I} , Ga^{I} , In^{I} or Tl^{I} by heating with a suitable molten salt, and Ag^{I} can be replaced by NO^+ by treatment with molten $\text{NOCl}/\text{AlCl}_3$. The ammonium compound is also known and H_3O^+ - β -alumina can be prepared by reduction of the Ag compound. Similarly, Al^{III} can be replaced by Ga^{III} or Fe^{III} in the preparation, leading to compounds of (idealized) formulae $\text{Na}_2\text{O} \cdot 11\text{Ga}_2\text{O}_3$, $\text{Na}_2\text{O} \cdot 11\text{Fe}_2\text{O}_3$, $\text{K}_2\text{O} \cdot 11\text{Fe}_2\text{O}_3$, etc. Altrivalent substitution is also possible, e.g. in Na- β'' -alumina, $\text{Na}_{1+x}\text{M}_x\text{Al}_{1-x}\text{O}_{17}$, in which M is a

divalent cation such as Mg, Ni or Zn. A typical composition is $\text{Na}_{1.67}\text{Mg}_{0.67}\text{Al}_{10.33}\text{O}_{17}$ and the excess Na charge is compensated for by substituting the divalent or univalent cation into the lattice sites normally occupied by Al.⁽⁵⁸⁾

Apart from the intriguing structural implications of these fast-ion solid-state conductors, Na- β -alumina and related phases have been extensively used as permeable membranes in the Na/S battery system (p. 678): this requires an air-stable membrane that is readily permeable to Na ions but not to Na atoms or S, that is non-reactive with molten Na and S, and that is not an electronic conductor. Not surprisingly, few compounds have been found to compete with Na- β -alumina in this field, although Na- β'' -alumina has the remarkable additional property of enabling the rapid diffusion of a large proportion of cations in the periodic table (whereas Na- β -alumina itself is restricted mainly to univalent cations). Indeed, the β'' -aluminas are the first family of high conductivity solid electrolytes which permit fast ion transport of multivalent cations in solids.⁽⁵⁸⁾

Unrelated to the β - and β'' -aluminas are a group of white, hygroscopic sodium-rich aluminates which have recently been prepared by heating Na_2O and Al_2O_3 in appropriate stoichiometric ratios at 700°C for 18–24 hours.⁽⁵⁹⁾ Na_5AlO_4 , which is isostructural with Na_5FeO_4 , contains isolated $[\text{AlO}_4]$ tetrahedra with Al–O 176–179 pm. $\text{Na}_7\text{Al}_3\text{O}_8$ features a novel ring structure made up of six AlO_4 tetrahedra sharing corners to form a non-planar 12-membered ring which is then joined by pairs of oxygen atom bridges to adjacent rings, thus generating an infinite chain of alternating 12- and 8-membered rings with Al–O $_{\mu}$ 175–179 pm and Al–O $_{\text{t}}$ 173–4 pm. Finally, $\text{Na}_{17}\text{Al}_5\text{O}_{16}$ has discrete chains composed of five AlO_4 tetrahedra sharing corners with almost linear angles (160° and 173°) at the bridging O atoms and with

⁵⁸ D. F. SHRIVER and G. C. FARRINGTON, *Chem. and Eng. News*, May 20, 42–57 (1985), and references cited therein.

⁵⁹ M. G. BARKER, P. G. GADD and M. J. BEGLEY, *J. Chem. Soc., Chem. Commun.*, 379–81 (1981). M. G. BARKER, P. G. GADD and S. C. WALLWORK, *J. Chem. Soc., Chem. Commun.*, 516–7 (1982).

the various Al–O distances again falling in the range 170–180 pm. Note that the unusual formula $\text{Na}_{17}\text{Al}_5\text{O}_{16}$ (i.e. $\text{Na}_{3.4}\text{AlO}_{3.2}$) is nearly the same as Na_3AlO_3 which would have been the stoichiometry if the chains of AlO_4 tetrahedra had been infinite.

Tricalcium aluminate, $\text{Ca}_3\text{Al}_2\text{O}_6$

Tricalcium aluminate is an important component of Portland cement yet, despite numerous attempts dating back over the preceding 50 y, its structure remained unsolved until 1975.⁽⁶⁰⁾ The basic unit is now known to be a 12-membered ring of 6 fused $\{\text{AlO}_4\}$ tetrahedra $[\text{Al}_6\text{O}_{18}]^{18-}$ as shown in Fig. 7.16; there are 8 such rings per unit cell surrounding holes of radius 147 pm, and the rings are held together by Ca ions in distorted sixfold coordination to give the structural formula $\text{Ca}_9\text{Al}_6\text{O}_{18}$. The rather short Ca–O distance (226 pm) and the observed compression of the $\{\text{CaO}_6\}$ octahedra may indicate some strain and this, together with the large holes in the lattice, facilitate the rapid reaction with water. The products of hydration depend sensitively on the temperature. Above 21° $\text{Ca}_3\text{Al}_2\text{O}_6$ gives the hexahydrate $\text{Ca}_3\text{Al}_2\text{O}_6 \cdot 6\text{H}_2\text{O}$, but below this temperature hydrated di- and tetra-calcium aluminates are formed of empirical composition $2\text{CaO} \cdot \text{Al}_2\text{O}_3 \cdot 5-9\text{H}_2\text{O}$ and $4\text{CaO} \cdot \text{Al}_2\text{O}_3 \cdot 12-14\text{H}_2\text{O}$. This is of great importance in cement technology (see Panel) since, in the absence of a retarder, cement reacts rapidly with water giving a sharp rise in temperature and a “flash set” during which the various calcium aluminate hydrates precipitate and congeal into an unmanageable mass. This can be avoided by grinding in 2–5% of gypsum ($\text{CaSO}_4 \cdot 2\text{H}_2\text{O}$) with the cement clinker; this reacts rapidly with dissolved aluminates in the presence of $\text{Ca}(\text{OH})_2$ to give the calcium sulfatoaluminate, $3\text{CaO} \cdot \text{Al}_2\text{O}_3 \cdot 3\text{CaSO}_4 \cdot 31\text{H}_2\text{O}$, which is much less soluble than the hydrated calcium aluminates and

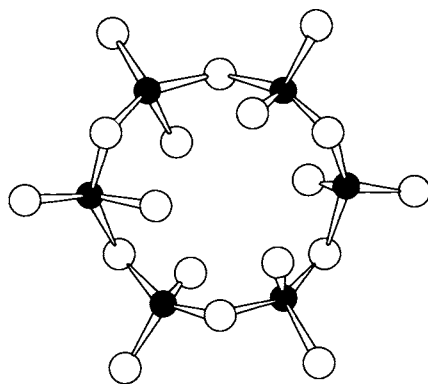


Figure 7.16 Structure of the $[\text{Al}_6\text{O}_{18}]^{18-}$ unit in $\text{Ca}_3\text{Al}_2\text{O}_6$ (i.e. $\text{Ca}_9\text{Al}_6\text{O}_{18}$). The Al–O distances are all in the range 175 ± 2 pm.

therefore preferentially precipitates and prevents the premature congealing.

Another important calcium aluminate system occurs in high-alumina cement (*ciment fondu*). This is not a Portland cement but is made by fusing limestone and bauxite with small amounts of SiO_2 and TiO_2 in an open-hearth furnace at 1425–1500°; rotary kilns with tap-holes for the molten cement can also be used. Typical analytical compositions for a high-alumina cement are ~40% each of Al_2O_3 and CaO and about 10% each of Fe_2O_3 and SiO_2 ; the most important compounds in the cement are CaAl_2O_4 , $\text{Ca}_2\text{Al}_2\text{SiO}_7$ and $\text{Ca}_6\text{Al}_8\text{FeSiO}_{21}$. Setting and hardening of high-alumina cement are probably due to the formation of calcium aluminate gels such as $\text{CaO} \cdot \text{Al}_2\text{O}_3 \cdot 10\text{H}_2\text{O}$, and the more basic $2\text{CaO} \cdot \text{Al}_2\text{O}_3 \cdot 8\text{H}_2\text{O}$, $3\text{CaO} \cdot \text{Al}_2\text{O}_3 \cdot 6\text{H}_2\text{O}$ and $4\text{CaO} \cdot \text{Al}_2\text{O}_3 \cdot 13\text{H}_2\text{O}$, though these empirical formulae give no indication of the structural units involved. The most notable property of high-alumina cement is that it develops very high strength at a very early stage (within 1 day). Long exposure to warm, moist conditions may lead to failure but resistance to corrosion by sea water and sulfate brines, or by weak mineral acids, is outstanding. It has also been much used as a refractory cement to withstand temperatures up to 1500°.

⁶⁰ P. MONDAL and J. W. JEFFREY, *Acta Cryst.* **B31**, 689–97 (1975).

Portland Cement⁽⁶¹⁾

The name "Portland cement" was first used by J. Aspdin in a patent (1824) because, when mixed with water and sand the powder hardened into a block that resembled the natural limestone quarried in the Isle of Portland, England. The two crucial discoveries which led to the production of strong, durable, hydraulic cement that did not disintegrate in water, were made in the eighteenth and nineteenth centuries. In 1756 John Smeaton, carrying out experiments in connection with building the Eddystone Lighthouse (UK), recognized the importance of using limes which contained admixed clays or shales (i.e. aluminosilicates), and by the early 1800s it was realized that firing must be carried out at sintering temperatures in order to produce a clinker now known to contain calcium silicates and aluminates. The first major engineering work to use Portland cement was in the tunnel constructed beneath the Thames in 1828. The first truly high-temperature cement (1450–1600°C) was made in 1854, and the technology was revolutionized in 1899 by the introduction of rotary kilns.

The important compounds in Portland cement are dicalcium silicate (Ca_2SiO_4) 26%, tricalcium silicate (Ca_3SiO_5) 51%, tricalcium aluminate ($\text{Ca}_3\text{Al}_2\text{O}_6$) 11% and the tetracalcium species $\text{Ca}_4\text{Al}_2\text{Fe}_2^{\text{III}}\text{O}_{10}$ (1%). The principal constituent of moistened cement paste is a tobermorite gel which can be represented schematically by the following idealized equations:



The adhesion of the tobermorite particles to each other and to the embedded aggregates is responsible for the strength of the cement which is due, ultimately, to the formation of $-\text{Si}-\text{O}-\text{Si}-\text{O}$ bonds.

Portland cement is made by heating a mixture of limestone (or chalk, shells, etc.) with aluminosilicates (derived from sand, shales, and clays) in carefully controlled amounts so as to give the approximate composition $\text{CaO} \sim 70\%$, $\text{SiO}_2 \sim 20\%$, $\text{Al}_2\text{O}_3 \sim 5\%$, $\text{Fe}_2\text{O}_3 \sim 3\%$. The presence of Na_2O , K_2O , MgO and P_2O_5 are detrimental and must be limited. The raw materials are ground to pass 200-mesh sieves and then heated in a rotary kiln to $\sim 1500^\circ$ to give a sintered clinker; this is reground to 325-mesh and mixed with 2–5% of gypsum. An average-sized kiln can produce 1000–3000 tonnes of cement per day and the world's largest plants can produce up to 8000 tonnes per day. The vast scale of the industry can be gauged from the US production figures in the table below. Price (1990) was \$45–55 per tonne for bulk supplies. In the same year China emerged as the world's largest cement producer (200 million tonnes per annum). Total world production continues to grow dramatically, from 590 Mtpa in 1970 and 881 Mtpa in 1980 to nearly 1200 Mtpa in 1990, of which Europe (including the European parts of the former Soviet Union) accounted for some 40%.

Production of Portland Cement in the USA/million tonnes (Mt)

1890	1900	1910	1920	1930	1940	1950	1960	1970	1980	1990
0.057	1.45	13.1	17.1	27.5	22.2	38.5	56.0	66.4	68.2	70.0

7.3.5 Other inorganic compounds

Chalcogenides

At normal temperatures the only stable chalcogenides of Al are Al_2S_3 (white), Al_2Se_3 (grey) and Al_2Te_3 (dark grey). They can be prepared by direct reaction of the elements at $\sim 1000^\circ$ and all hydrolyse rapidly and completely in aqueous solution to give $\text{Al}(\text{OH})_3$ and H_2X ($\text{X} = \text{S}, \text{Se}, \text{Te}$). The small size of Al relative to the chalcogens dictates tetrahedral coordination and the various polymorphs are related to wurtzite (hexagonal ZnS , p. 1210), two-thirds of the available

metal sites being occupied in either an ordered (α) or a random (β) fashion. Al_2S_3 also has a γ -form related to $\gamma\text{-Al}_2\text{O}_3$ (p. 243), and very recently a novel high-temperature hexagonal modification of Al_2S_3 containing 5-coordinate Al has been obtained by annealing $\alpha\text{-Al}_2\text{S}_3$ at 550°C ;⁽⁶²⁾ in this new form half the Al atoms are tetrahedrally coordinated ($\text{Al}-\text{S}_{223} = 227$ pm) whereas the other half are in trigonal bipyramidal coordination with $\text{Al}-\text{S}_{\text{eq}} = 227\text{--}232$ pm and $\text{Al}-\text{S}_{\text{ax}} = 250\text{--}252$ pm.

The chalcogenides of Ga, In and Tl are much more numerous and at least a dozen different structure types have been established by X-ray

⁶¹ Kirk-Othmer Encyclopedia of Chemical Technology, 4th edn., Vol. 5, Interscience, New York, 564–98 (1993).

⁶² B. KREBS, A. SCHIEMANN and M. LAGE, *Z. anorg. allg. Chem.* **619**, 983–8 (1993).

crystallography.⁽⁶³⁾ The compounds have been extensively studied not only because of their intriguing stoichiometries, but also because many of them are semiconductors, semi-metals, photoconductors or light emitters, and Tl_5Te_3 has been found to be a superconductor at low temperatures. (See p. 1182 for high-temperature superconductors, including $Tl_2Ca_2Ba_2Cu_3O_{10+x}$ which has one of the highest known superconducting transition temperatures, $T_c = 125$ K.) The chalcogenides, as expected from their position in the

periodic table, are far from ionic, but formal oxidation states remain a useful device for electron counting and for checking the overall charge balance. Well-established compounds are summarized in Table 7.9. The following points are noteworthy. The hexagonal α - and β -forms of Ga_2S_3 are isostructural with the Al analogues and an additional form, γ - Ga_2S_3 , adopts the related defect sphalerite structure derived from cubic ZnS (zinc blende, p. 1210). The same structure is found for Ga_2Se_3 and Ga_2Te_3 but for the larger In^{III} atom octahedral coordination also becomes possible. The corresponding Tl^{III} sesquichalcogenides Tl_2X_3 are either

⁶³ L. I. MAN, R. M. IMANOV and S. A. SEMILETOV, *Sov. Phys. Crystallogr.* **21**, 255–63 (1976).

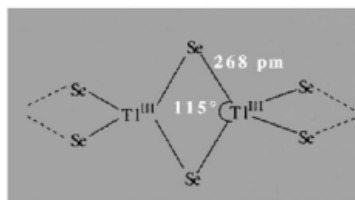
Table 7.9 Stoichiometries and structures of the crystalline chalcogenides of Group 13 elements

Ga_2S	Ga_2Se	
GaS (yellow) layer structure with Ga–Ga bonds	$GaSe$ (like GaS)	$GaTe$ (like GaS)
Ga_4S_5		(Ga_3Te_2)
α - Ga_2S_3 (yellow) ordered defect wurtzite (hexagonal ZnS)		
β - Ga_2S_3 defect wurtzite		
γ - Ga_2S_3 defect sphalerite (cubic ZnS)	Ga_2Se_3 defect sphalerite	Ga_2Te_3 defect sphalerite
		Ga_2Te_5 chains of linked $\{GaTe_4\}$ plus single Te atoms
	In_4Se_3 contains $[(In^{III})_3]^V$ groups: $In^I[In_3^{III}]Se_3$	In_4Te_3 like In_4Se_3
InS (red) like GaS	$InSe$ distorted NaCl, somewhat like GaS	$InTe$ like $TlSe$ (cubes and tetrahedra)
In_6S_7 see text	In_6Se_7 like In_6S_7	In_3Te_4
α - In_2S_3 (yellow) cubic γ' - Al_2O_3	α - In_2Se_3 defect wurtzite, but $\frac{1}{16}$ of In octahedral	α - In_2Te_3 defect sphalerite (cubic ZnS)
β - In_2S_3 (red) defect spinel, γ - Al_2O_3	β - In_2Se_3 ordered defect wurtzite (hexagonal ZnS)	β - In_2Te_3
In_6S_7 see text		In_3Te_5 In_2Te_5
Tl_2S (black) distorted CdI_2 layer lattice (Tl^I in threefold coordination)		
Tl_4S_3 chains of linked $\{Tl^{III}S_4\}$ tetrahedra $(Tl^I)_3[Tl^{III}S_3]$	Tl_5Se_3 complex Cr_5B_3 -type structure	Tl_5Te_3 Cr_5B_3 layer structure, CN of Tl varies up to 9 and Te up to 10
TlS (black) like $TlSe$, $Tl^I[Tl^{III}S_2]$	$TlSe$ (black) chains of edgeshared $\{Tl^{III}Se_4\}$ tetrahedra $Tl^I[Tl^{III}Se_2]$	$TlTe$ variant of W_5Si_3 (complex)
[No Tl_2S_3 known]	Tl_2Se_3	(Tl_2Te_3)
TlS_2 Tl^I polysulfide		
Tl_2S_5 (red and black forms) Tl^I polysulfide		
Tl_2S_9 Tl^I polysulfide		

non-existent or of dubious authenticity, perhaps because of the ready reduction to Tl^I (see TlI_3 , p. 239).

GaS (yellow, mp 970°) has a hexagonal layer structure with $Ga-Ga$ bonds (248 pm); each Ga is coordinated by 3S and 1Ga, and the sequence of layers along the c -axis is $\cdots SGaGaS, SGaGaS \cdots$; the compound can therefore be considered as an example of Ga^{II} . The structures of $GaSe$, $GaTe$, red InS and $InSe$ are similar. By contrast, $InTe$, TlS (black) and $TlSe$ (black, metallic) have a structure which can be formalized as $M^I[M^{III}X_2]$; each Tl^{III} is tetrahedrally coordinated by 4 Se at 268 pm and the tetrahedra are linked into infinite chains by edge sharing along the c -axis (see structure), whereas each Tl^I lies between these chains and is surrounded by a distorted cube of 8 Se at 342 pm. This explains the marked anisotropy of properties, especially the metallic conductivity in the (001) plane and the semiconductivity along the c -axis. Similar edge-linked $\{GeSe_4\}$ tetrahedra are found in $Cs_{10}Ga_6Se_{14}$ which was obtained as transparent pale-yellow crystals by heating an equimolar mixture of $GaSe$ and Cs in a carefully controlled temperature programme; the compound features the unprecedented finite complex anion $[Se_2Ga(\mu-Se_2Ga)_5Se_2]^{10-}$ which is 1900 pm long.⁽⁶⁴⁾

⁶⁴ H. J. DEISEROTH and HAN FU-SON, *Angew. Chem. Int. Edn. Engl.* **20**, 962-3 (1981).



In_6S_7 (and the isostructural In_6Se_7) have a curious structure comprising two separate blocks of almost ccp S which are rotated about the b -axis by 61° with respect to each other; the In is in octahedral coordination. The compound can be formulated as $In^I(In_2^{III})^{IV}In_3^{III}S_7^{-II}$. There are also numerous ternary In/Tl sulfides in which In^I has been replaced by Tl^I , e.g.: $Tl^IIn_3^{III}S_8$, $Tl^IIn_3^{III}S_5$, $Tl^IIn^{III}S_2$, $Tl_3In^{III}S_3$, $Tl^I(In_2^{III})_2^{IV}In^{III}S_6$, $Tl_3^IIn^IIn_4^{III}S_8$ and $Tl^I(In_2^{III})^{IV}In_3^{III}S_7$.^(64a)

The crystal structures of In_4Se_3 and In_4Te_3 show that they can be regarded to a first approximation as $In^I[In_3]^V(X^{-II})_3$ but the compound does not really comprise discrete ions. The triatomic unit $[In^{III}-In^{III}-In^{III}]$ is bent, the angle at the central atom being 158° and the In-In distances 279 pm (cf. 324-326 pm in metallic In). However, it is also possible to discern non-planar 5-membered heterocycles in the structure formed by joining 2 In from 1 $\{In_3\}$ to the terminal In of an adjacent $\{In_3\}$ via 2 bridging Se (or Te) atoms so that the structure can be represented schematically as in Fig. 7.17. The $In^{III}-Se$ distances average

^{64a} H. J. DEISEROTH and R. WALTHER, *Z. anorg. allg. Chem.* **622**, 611-16 (1996).

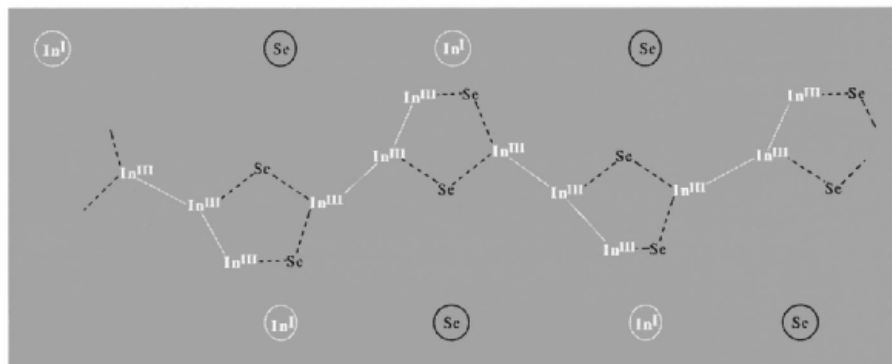


Figure 7.17 Schematic structure of In_4Se_3 .

269 pm compared with the closest In^I–Se contact of 297 pm. The [In^{III}]^V unit can be compared with the isoelectronic species [Hg₃^{II}]^{II}. The compound Tl₄S₃, which has the same stoichiometry as In₄X₃, has a different structure in which chains of corner-shared {Tl^{III}S₄} tetrahedra of overall stoichiometry [TlS₃] are bound together by Tl^I; within the chains the Tl^{III}–S distance is 254 pm whereas the Tl^I–S distances vary between 290–336 pm. A comparison of the formal designation of the two structures In^I[(In^{III})]^V(Se^{-II})₃ and (Tl^I)₃[Tl^{III}S₃]^{-III} again illustrates the increasing preference of the heavier metal for the +1 oxidation state. The trend continues with the polysulfides Tl^IS₂, Tl^IS₅ and Tl^IS₉, already alluded to on p. 253.

Compounds with bonds to N, P, As, Sb or Bi

The binary compounds of the Group 13 metals with the elements of Group 15 (N, P, As, Sb, Bi) are structurally less diverse than the chalcogenides just considered but they have achieved considerable technological application as III–V semiconductors isoelectronic with Si and Ge (cf. BN isoelectronic with C, p. 207). Their structures are summarized in Table 7.10: all adopt the cubic ZnS structure except the nitrides of Al, Ga and In which are probably more ionic (less covalent or metallic) than the others. Thallium does not form simple compounds

Table 7.10 Structures of III–V compounds MX^(a)

X ↓	M →	B	Al	Ga	In
N		L, S	W	W	W
P		S	S	S	S
As		S	S	S	S
Sb		—	S	S	S

^(a)L = BN layer lattice (p. 208).

S = sphalerite (zinc blende), cubic ZnS (p. 1210).

W = wurtzite, hexagonal ZnS structure (p. 1210).

M^{III}X^V: the explosive black nitride Tl₃N is known, and the azides Tl^IN₃ and Tl^I[Tl^{III}(N₃)₄]; the phosphides Tl₃P, TlP₃ and TlP₅ have been reported but are not well characterized. With As, Sb and Bi thallium forms alloys and intermetallic compounds Tl₃X, Tl₇Bi₂ and TlBi₂.

The III–V semiconductors can all be made by direct reaction of the elements at high temperature and under high pressure when necessary. Some properties of the Al compounds are in Table 7.11 from which it is clear that there are trends to lower mp and energy band-gap E_g with increasing atomic number.

Analogous compounds of Ga and In are grey or semi-metallic in appearance and show similar trends (Table 7.12). These data should be compared with those for Si, Ge, Sn and Pb on p. 373 and for the isoelectronic II–VI semiconductors of Zn, Cd and Hg with S, Se and Te (p. 1210). In addition, GaN is obtained by reacting Ga and NH₃ at 1050° and InN by reducing and nitriding In₂O₃ with NH₃ at 630°. The

Table 7.11 Some properties of Al III–V compounds

Property	AlN	AlP	AlAs	AlSb
Colour	Pale yellow	Yellow	Orange	—
MP/°C	>2200 decomp	2000	1740	1060
E_g /kJ mol ^{-1(a)}	411	236	208	145

^(a)Energy gap between top of (filled) valence band and bottom of (empty) conduction band (p. 332). To convert from kJ mol⁻¹ to eV atom⁻¹ divide by 96.485.

Table 7.12 Comparison of some III–V semiconductors

Property	GaP	GaAs	GaSb	InP	InAs	InSb
MP/°C	1465	1238	712	1070	942	525
E_g /kJ mol ^{-1(a)}	218	138	69	130	34	17

^(a)See note to Table 7.11.

nitrides show increasing susceptibility to chemical attack, AlN being inert to both acids and alkalis, GaN being decomposed by alkali, but not acid, and InN being decomposed by both acids and alkalis. Most of the other III–V compounds decompose slowly in moist air, e.g. AlP gives Al(OH)₃ and PH₃. As a consequence, semiconductor devices must be completely encapsulated to prevent reaction with the atmosphere. The great value of III–V semiconductors is that they extend the range of properties of Si and Ge and by judicious mixing in ternary phases they permit a continuous interpolation of energy band gaps, current-carrier mobilities and other characteristic properties. Some of their uses are summarized in the Panel on p. 258.

Other compounds containing Al–N or Ga–N bonds, including heterocyclic compounds and cluster organometallic compounds, are considered in section 7.3.6.

Some unusual stereochemistries

While it remains true that tetrahedral and octahedral coordination modes are the predominant stereochemistries adopted by the group 13 metals, nevertheless increasing diversity is being achieved by carefully selecting appropriate electronic and geometric features to enhance the stabilization of unusual stereochemistries. Some representative examples follow.

Trigonal planar Al is found in the [AlSb₃]⁶⁻ “anions” in [Cs₆K₃Sb(AlSb₃)], which is formed by heating a stoichiometric mixture of 6Cs, 3KSb and AlSb in a sealed Nb ampoule at 677°C.⁽⁶⁵⁾ The Ga analogue was prepared similarly. The planar anions are embedded between columns of condensed icosahedra (Cs₆K_{6/2})⁹⁺ which in turn are centred by the remaining unique monatomic Sb³⁻ anion.

The indium molybdate In₁₁Mo₄₀O₆₂, prepared by heating the appropriate mixture of In, Mo and MoO₂ at 1100°C, features novel quasi-linear chain cations. In₅⁷⁺ and In₆⁸⁺ in channels

between condensed clusters of Mo₆ octahedra.⁽⁶⁶⁾ The intrachain distances are 262–266 pm in In₅⁷⁺ and 265–269 pm in In₆⁸⁺, which are the shortest known In–In interatomic distances cf. 325 and 337 pm in In metal itself, and 333 pm for the closest distances between In atoms in neighbouring chains in the molybdate. Interatomic angles within the chains are 158° and 163° respectively and, when the coordination around each In atom by contiguous In and O atoms is considered, the chains can be formulated as [In²⁺(In⁺)_nIn²⁺], *n* = 3, 4.

Square-pyramidal 5-coordinate In^{III} occurs in certain organoindium compounds such as the bis(2-methylaminopyridino-) adduct [MeIn{MeNC(CH₃)₄N}]₂⁽⁶⁷⁾ — cf. InCl₅²⁻ (p. 238). The less familiar pentagonal planar coordination has been established for the InMn₅ group in the dianion [(μ₅-In){Mn(CO)₄]₅]²⁻ which is readily prepared by treatment of InCl₃ with the manganese carbonyl cluster compound K₃[Mn₃(μ-CO)₂(CO)₁₀].⁽⁶⁸⁾ The mean Mn–Mn distance in the encircling plane-pentagonal “ligand” {Mn(CO)₄]₅ is 317 pm; the mean In–Mn distance is 265 pm, and the In atom is only 4.6 pm from the best plane of the five Mn atoms. Note also that the ligand is isolobal with cyclopentadienyl, C₅H₅.

Seven-coordinate pentagonal-bipyramidal In^{III} has been found in the chloroindium complex of 1,4,7-triazacyclononane triacetic acid [{"-(CH₂)₂N(CH₂CO₂H)}]₃}, (LH₃).⁽⁶⁹⁾ The neutral, monoprotinated 7-coordinate complex [InCl(LH)] features Cl and one N in axial positions (angle Cl–In–N 168°) with the other two N atoms and three carboxylate O atoms in the pentagonal plane. Interest in such compounds stems

⁶⁶ H. MATTAUSCH, A. SIMON and E.-M. PETERS, *Inorg. Chem.* **25**, 3428–33 (1986).

⁶⁷ A. M. ARIA, D. C. BRADLEY, D. M. FRIGO, M. B. HURSTHOUSE and B. HUSSAIN, *J. Chem. Soc., Chem. Commun.*, 783–4 (1985).

⁶⁸ M. SCHOLLENBERGER, B. NUBER and M. L. ZIEGLER, *Angew. Chem. Int. Edn. Engl.* **31**, 350–1 (1992).

⁶⁹ A. S. CRAIG, I. M. HELPS, D. PARKER, H. ADAMS, N. A. BAILEY, M. G. WILLIAMS, J. M. A. SMITH and G. FERGUSON, *Polyhedron* **8**, 2481–4 (1989).

⁶⁵ M. SOMER, K. PETERS, T. POPP and H. G. VON SCHNERING, *Z. anorg. allg. Chem.* **597**, 201–8 (1991).

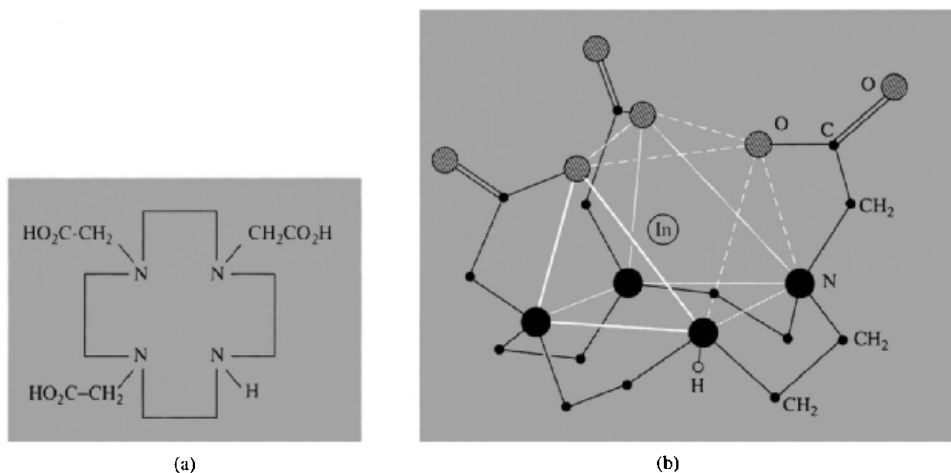


Figure 7.18 (a) 1,4,7,10-tetraazacyclododecane triacetic acid, (LH_3). (b) Structure of the 7-coordinate complex $[InL]$; the coordination polyhedron (shown in white) comprises a trigonal prism of 4N and 2O capped on one of its quadrilateral faces by the third O atom.

from the use of the γ -active ^{111}In isotope (E_γ 173, 247 keV, $t_{1/2}$ 2.81 d) in radio-labelled monoclonal antibodies to detect tumours. Interestingly, the 7-coordinate crystalline complex reverts to a stable neutral hexacoordinate species in aqueous solution. Other 7-coordinate macrocyclic In^{III} complexes of potential relevance in radio-pharmaceutical applications have been prepared, including $[InL]$ where L is the triacetate of the tetraaza macrocycle shown in Fig. 7.18(a).⁽⁷⁰⁾ In this case the coordination polyhedron is a trigonal prism with one of its quadrilateral faces capped by a carboxylate O atom as shown schematically in Fig. 7.18(b).

Indium clusters have also recently been characterized, notably in intermetallic compounds. Thus, the Zintl phase, Rb_2In_3 , (prepared by direct reaction between the two metals at $1530^\circ C$) has layers of octahedral *closo*- In_6 clusters joined into sheets through exo bonds at four coplanar vertices.⁽⁷¹⁾ These four In atoms are therefore each bonded to five neighbouring In atoms at the corners of a square-based pyramid, whereas the remaining two (*trans*) In atoms in the In_6 cluster

show pyramidal 4-fold bonding only, to contiguous In atoms in the same cluster. Cs_2In_3 is isostructural. The intermetallic compound $K_3Na_{26}In_{48}$ (synthesized from the elements in sealed Nb ampoules at $600^\circ C$) has a more complicated structure in which the In forms both *closo* icosahedral In_{12} clusters and hexagonal antiprismatic In_{12} clusters.⁽⁷²⁾ All the various In_{12} clusters are interconnected by 12 exo bonds forming a covalent 3D network (In–In 291–315 pm) and the In_{12} hexagonal antiprisms are additionally centred by single Na atoms. The phase contains several other interesting structural features and the original paper (in English) makes rewarding reading.

7.3.6 Organometallic compounds

Many organoaluminium compounds are known which contain 1, 2, 3 or 4 Al–C bonds per Al atom and, as these have an extensive reaction chemistry of considerable industrial importance, they will be considered before the organometallic compounds of Ga, In and Tl are discussed.

⁷⁰ A. RIESEN, T. A. KADEN, W. RITTER and H. A. MACKE, *J. Chem. Soc., Chem. Commun.*, 460–2 (1989).

⁷¹ S. C. SEVEOV and J. D. CORBETT, *Z. anorg. allg. Chem.* **619**, 128–32 (1993).

⁷² W. CARRILLO-CABRERA, N. CAROCA-CANALES, K. PETERS and H. G. VON SCHNERING, *Z. anorg. allg. Chem.* **619**, 1556–63 (1993).

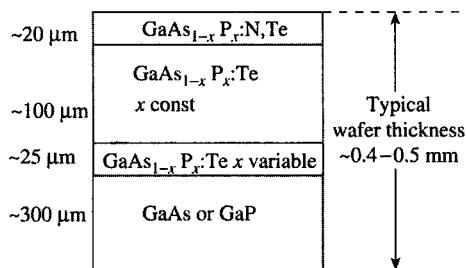
Organoaluminium Compounds

Aluminium trialkyls and triaryls are highly reactive, colourless, volatile liquids or low-melting solids which ignite spontaneously in air and react violently with water; they should therefore be handled circumspectly and with

suitable precautions. Unlike the boron trialkyls and triaryls they are often dimeric, though with branched-chain alkyls such as Pr^i , Bu^i and Me_3CCH_2 this tendency is less marked. Al_2Me_6 (mp 15° , bp 126°) has the methyl-bridged structure shown and the same dimeric structure is found for Al_2Ph_6 (mp 225°).

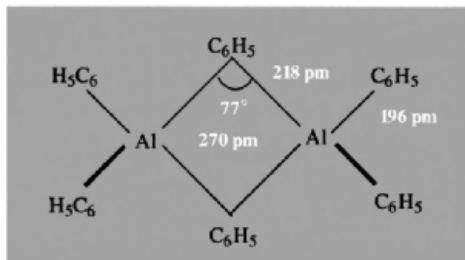
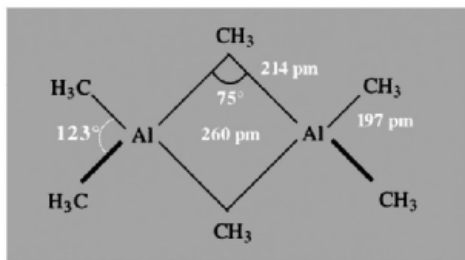
Applications of III-V Semiconductors

The 9 compounds that Al, Ga and In form with P, As and Sb have been extensively studied because of their many applications in the electronics industry, particularly those centred on the interconversion of electrical and optical (light) energy. For example, they are produced commercially as light-emitting diodes (LEDs) familiar in pocket calculators, wrist watches and the alpha-numeric output displays of many instruments; they are also used in infrared-emitting diodes, injection lasers, infrared detectors, photocathodes and photomultiplier tubes. An extremely elegant chemical solid-state technology has evolved in which crystals of the required properties are deposited, etched and modified to form the appropriate electrical circuits. The ternary system $\text{GaAs}_{1-x}\text{P}_x$ now dominates the LED market for α -numeric and graphic displays following the first report of this activity in 1961. $\text{GaAs}_{1-x}\text{P}_x$ is grown epitaxially on a single-crystal substrate of GaAs or GaP by chemical vapour deposition and crystal wafers as large as 20 cm^2 have been produced commercially. The colour of the emitted radiation is determined by the energy band gap E_g ; for GaAs itself E_g is 138 kJ mol^{-1} corresponding to an infrared emission (λ 870 nm), but this increases to 184 kJ mol^{-1} for $x \sim 0.4$ corresponding to red emission (λ 650 nm). For $x > 0.4$ E_g continues to increase until it is 218 kJ mol^{-1} for GaP (green, λ 550 nm). Commercial yellow and green LEDs contain the added isoelectronic impurity N to improve the conversion efficiency. A schematic cross-section of a typical $\text{GaAs}_{1-x}\text{P}_x$ epitaxial wafer doped with Te and N is shown in the diagram: Te (which has one more valence electron per atom than As or P) is the most widely used dopant to give n -type impurities in this system at concentrations of 10^{16} – 10^{18} atoms cm^{-3} (0.5–50 ppm). The p - n junction is then formed by diffusing Zn (1 less electron than Ga) into the crystal to a similar concentration.



An even more recent application is the construction of semiconductor lasers. In normal optical lasers light is absorbed by an electronic transition to a broad band which lies above the upper laser level and the electron then drops into this level by a non-radiative transition. By contrast the radiation in a semiconductor laser originates in the region of a p - n junction and is due to the transitions of injected electrons and holes between the low-lying levels of the conduction band and the uppermost levels of the valence band. (Impurity levels may also be involved.) The efficiency of these semiconductor injection lasers is very much higher than those of optically pumped lasers and the devices are much smaller; they are also easily adaptable to modulation. As implied by the band gaps on p. 255, emission wavelengths are in the visible and near infrared. A heterostructure laser based on the system $\text{GaAs}-\text{Al}_x\text{Ga}_{1-x}\text{As}$ was the first junction laser to run continuously at 3000 K and above (1970).

In the two types of device just considered, namely light emitting diodes and injection lasers, electrical energy is converted into optical energy. The reverse process of converting optical energy into electrical energy (photoconductivity and photovoltaic effects) has also been successfully achieved by III-V semiconductor systems. For example, the small band-gap compound InSb is valuable as a photoconductive infrared detector, and several compounds are being actively studied for use in solar cells to convert sunlight into useful sources of electrical power. The maximum photon flux in sunlight occurs at 75 – 95 kJ mol^{-1} and GaAs shows promise, though other factors make $\text{Cu}_2\text{S}-\text{CdS}$ cells more attractive commercially at the present time.

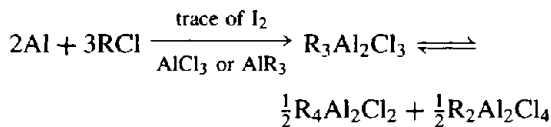


In each case $\text{Al}-\text{C}_\mu$ is about 10% longer than $\text{Al}-\text{C}_t$ (cf. Al_2X_6 , p. 235; B_2H_6 , p. 157). The enthalpy of dissociation of Al_2Me_6 into monomers is 84 kJ mol^{-1} . Al_2Et_6 (mp -53°) and Al_2Pr_6 (mp -107°) are also dimeric at room temperature but crystalline trimesitylaluminium (mesityl = 2,4,5-trimethylphenyl) is monomeric with planar 3-coordinate Al; the mesityl groups adopt a propeller-like configuration with a dihedral angle of 56° between the aromatic ring and the AlC_3 plane and with $\text{Al}-\text{C}$ 199.5 pm.⁽⁷³⁾

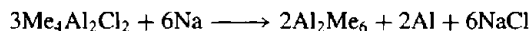
As with $\text{Al}(\text{BH}_4)_3$ and related compounds (p. 230), solutions of Al_2Me_6 show only one proton nmr signal at room temperature due to the rapid interchange of bridging and terminal Me groups; at -75° this process is sufficiently slow for separate resonances to be observed.

Al_2Me_6 can be prepared on a laboratory scale by the reaction of HgMe_2 on Al at $\sim 90^\circ\text{C}$. Al_2Ph_6 can be prepared similarly using HgPh_2 in boiling toluene or by the reaction of LiPh on Al_2Cl_6 . On the industrial (kilotonne) scale Al is alkylated by means of RX or by alkenes plus H_2 . In the first method the sesquichloride $\text{R}_3\text{Al}_2\text{Cl}_3$ is formed in equilibrium with its disproportionation

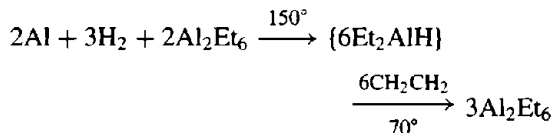
products:[†]



Addition of NaCl removes $\text{R}_2\text{Al}_2\text{Cl}_4$ as the complex $(2\text{NaAlCl}_3\text{R})$ and enables $\text{R}_4\text{Al}_2\text{Cl}_2$ to be distilled from the mixture. Reaction with Na yields the trialkyl, e.g.:



Higher trialkyls are more readily prepared on an industrial scale by the alkene route (K. Ziegler *et al.*, 1960) in which H_2 adds to Al in the presence of preformed AlR_3 to give a dialkylaluminium hydride which then readily adds to the alkene:



Similarly, Al, H_2 and $\text{Me}_2\text{C}=\text{CH}_2$ react at 100° and 200 atm to give AlBu_3^i in a single-stage process, provided a small amount of this compound is present at the start; this is required because Al does not react directly with H_2 to form AlH_3 prior to alkylation under these conditions. Alkene exchange reactions can be used to transform AlBu_3^i into numerous other trialkyls. AlBu_3^i can also be reduced by potassium metal in hexane at room temperature to give the novel brown compound $\text{K}_2\text{Al}_2\text{Bu}_6^i$ (mp 40°) which is notable in providing a rare example of an Al-Al bond in the diamagnetic anion $[\text{Bu}_3^i\text{AlAlBu}_3^i]^{2-}$.⁽⁷⁴⁾

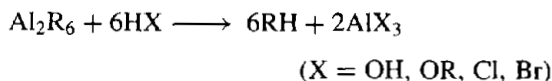
Al_2R_6 (or AlR_3) react readily with ligands to form adducts, LAlR_3 . They are stronger Lewis acids than are organoboron compounds, BR_3 , and can be considered as 'hard' (or class a)

[†] It is interesting to note that the reaction of EtI with Al metal to give the sesqui-iodide "Et₃Al₂I₃" was the first recorded preparation of an organoaluminium compound (W. Hallwachs and A. Schafarik, 1859).

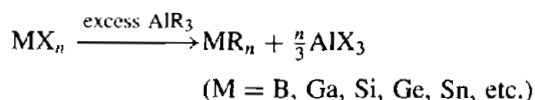
⁷⁴ H. HOBERG and S. KRAUSE, *Angew. Chem. Int. Edn. Engl.* **17**, 949-50 (1979).

⁷³ J. J. JERIUS, J. M. HAHN, A. F. M. M. RAHMAN, O. MOLS, W. H. ISLEY and J. P. OLIVER, *Organometallics* **5**, 1812-14 (1986).

acids; for example, the stability of the adducts AlMe_3 decreases in the following sequence of L: $\text{Me}_3\text{N} > \text{Me}_3\text{P} > \text{Me}_3\text{As} > \text{Me}_2\text{O} > \text{Me}_2\text{S} > \text{Me}_2\text{Se}$. With protonic reagents they react to liberate alkanes:

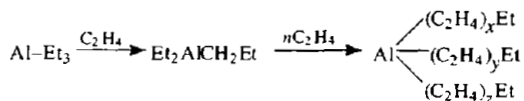


Reaction with halides or alkoxides of elements less electropositive than Al affords a useful route to other organometallics:



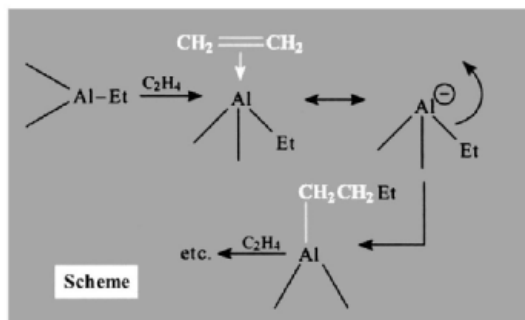
The main importance of organoaluminium compounds stems from the crucial discovery of alkene insertion reactions by K. Ziegler,⁽⁷⁵⁾ and an industry of immense proportions based on these reactions has developed during the past 40 y. Two main processes must be distinguished: (a) "growth reactions" to synthesize unbranched long-chain primary alcohols and alkenes (K. Ziegler *et al.*, 1955), and (b) low-pressure polymerization of ethene and propene in the presence of organometallic mixed catalysts (1955) for which K. Ziegler (Germany) and G. Natta (Italy) were jointly awarded the Nobel Prize for Chemistry in 1963.

In the first process alkenes insert into the Al-C bonds of monomeric AlR_3 at $\sim 150^\circ$ and 100 atm to give long-chain derivatives whose composition can be closely controlled by the temperature, pressure and contact time:

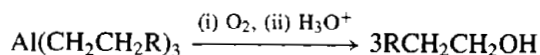


The reaction is thought to occur by repeated η^2 -coordination of ethene molecules to Al followed by migration of an alkyl group from Al to the alkene carbon atom (see Scheme).

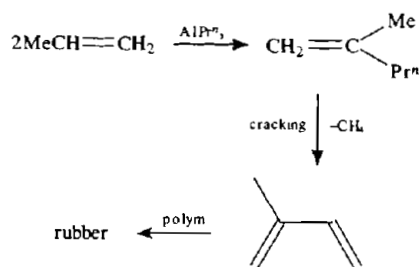
Unbranched chains up to C_{200} can be made, but prime importance attaches to chains of 14–20 C



atoms which are synthesized industrially in this way and then converted to unbranched aliphatic alcohols for use in the synthesis of biodegradable detergents:



Alternatively, thermolysis yields the terminal alkene $\text{RCH}=\text{CH}_2$. Note that, if propene or higher alkenes are used instead of ethene, then only single insertion into Al-C occurs. This has been commercially exploited in the catalytic dimerization of propene to 2-methylpentene-1, which can then be cracked to isoprene for the production of synthetic rubber (*cis*-1,4-polyisoprene):



Even more important is the stereoregular catalytic polymerization of ethene and other alkenes to give high-density polyethene ("polythene") and other plastics. A typical Ziegler-Natta catalyst can be made by mixing TiCl_4 and Al_2Et_6 in heptane: partial reduction to Ti^{III} and alkyl transfer occur, and a brown suspension forms which rapidly absorbs and polymerizes ethene even at room temperature and atmospheric pressure. Typical industrial conditions are 50–150°C and 10 atm. Polyethene

⁷⁵ K. ZIEGLER, *Adv. Organometallic Chem.* 6, 1–17 (1968).

produced at the surface of such a catalyst is 85–95% crystalline and has a density of 0.95–0.98 g cm⁻³ (compared with low-density polymer 0.92 g cm⁻³); the product is stiffer, stronger, has a higher resistance to penetration by gases and liquids, and has a higher softening temperature (140–150°). Polyethene is produced in megatonne quantities and used mainly in the form of thin film for packaging or as molded articles, containers and bottles; electrical insulation is another major application. Stereoregular (isotactic) polypropene and many copolymers of ethene are also manufactured. Much work has been done in an attempt to elucidate the chemical nature of the catalysts and the mechanism of their action; the active site may differ in detail from system to system but there is now general agreement that polymerization is initiated by η^2 coordination of ethene to the partly alkylated lower-valent transition-metal atom (e.g. Ti^{III}) followed by migration of the attached alkyl group from transition-metal to carbon (the Cossee mechanism, see Scheme below). An alternative suggestion involves a metal–carbene species generated by α -hydrogen transfer from carbon to the transition metal.⁽⁷⁶⁾

Coordination of the ethene or propene to Ti^{III} polarizes the C–C bond and allows ready migration of the alkyl group with its bonding electron-pair. This occurs as a concerted

process, and transforms the η^2 -alkene into a σ -bonded alkyl group. As much as 1 tonne of polypropylene can be obtained from as little as 5 g Ti in the catalyst.

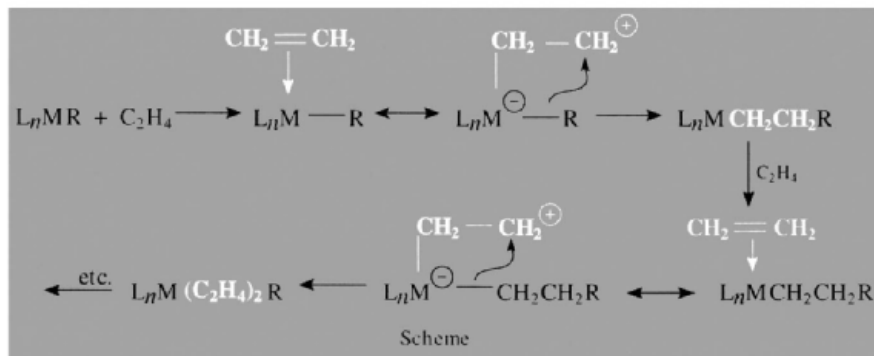
Finally, in this subsection, we mention a few recent examples of the use of specific ligands to stabilize particular coordination geometries about the organoaluminium atom (see also p. 256). Trigonal planar stereochemistry has been achieved in R₂AlCH₂AlR₂ {R = (Me₃Si)₂CH–}, which was prepared as colourless crystals by reacting CH₂(AlCl₂)₂ with 4 moles of LiCH(SiMe₃)₂ in pentane.⁽⁷⁷⁾ It is also noteworthy that the bulky R groups permit the isolation for the first time of a molecule having the AlCH₂Al grouping, by preventing the dismutation which spontaneously occurs with the Me and Et derivatives.

The linear cation [AlMe₂]⁺ has been stabilized by use of crown ethers (p. 96).⁽⁷⁸⁾ For example, 15-crown-5 gives overall pentagonal bipyramidal 7-fold coordination around Al with axial Me groups having Al–C 200 pm and angle Me–Al–Me 178° (see Fig. 7.19a). With the larger ligand 18-crown-6, the Al atom is bonded to only three of the six O atoms to give unsymmetrical 5-fold coordination with Al–C 193 pm and angle Me–Al–Me 141°. Symmetrical (square-pyramidal) 5-coordinate Al is found

⁷⁶ M. L. H. GREEN, *Pure Appl. Chem.* **50**, 27–35 (1978). K. J. IVIN, J. J. ROONEY, C. D. STEWART, M. L. H. GREEN and R. MAHTAB, *J. Chem. Soc., Chem. Commun.*, 604–6 (1978).

⁷⁷ M. LAYH and W. UHL, *Polyhedron* **9**, 277–82 (1990).

⁷⁸ S. G. BOTT, A. ALVANIPOUR, S. D. MORLEY, D. A. ATWOOD, C. M. MEANS, A. W. COLEMAN and J. L. ATWOOD, *Angew. Chem. Int. Edn. Engl.* **26**, 485–6 (1987).



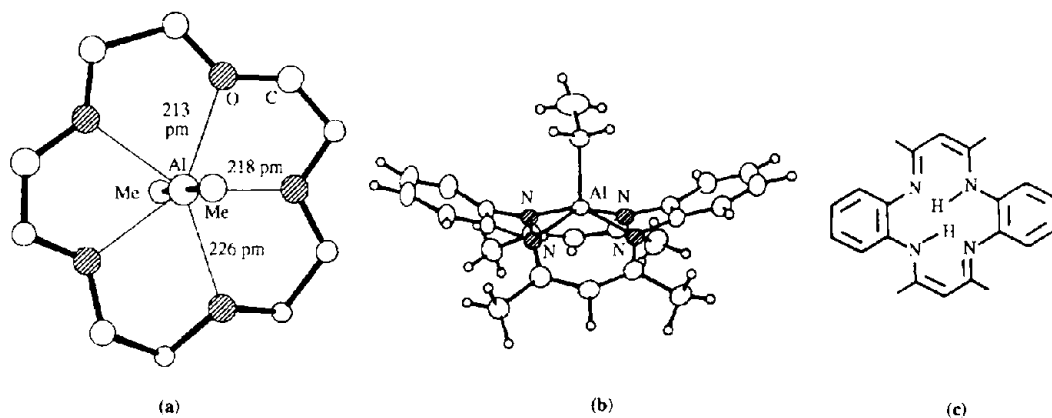


Figure 7.19 (a) Structure of the cation in $[\text{AlMe}_2(15\text{-crown-}5)]^+[\text{AlMe}_2\text{Cl}_2]^-$ showing pentagonal bipyramidal coordination of Al with axial Me groups. (b) Structure of $[\text{AlEtL}]$ where L is the bis(deprotonated) form of the macrocycle $\text{H}_2[\text{C}_{22}\text{H}_{22}\text{N}_4]$ shown in (c).

in the complex $[\text{AlEtL}]$ (Fig. 7.19b) formed by reacting Al_2Et_6 in hexane solution with $\text{H}_2[\text{C}_{22}\text{H}_{22}\text{N}_4]$, i.e. H_2L , shown in Fig. 7.19c.⁽⁷⁹⁾ The average Al–N distance is 196.7 pm, Al–C is 197.6 pm (close to the value for the terminal Al–C in Al_2Me_6 , p. 259) and the Al atom is 57 pm above the N_4 plane. A further notable feature is the great stability of the Al–C bond: the compound can be recrystallized unchanged from hydroxylic or water-containing solvents and does not decompose even when heated to 300°C in an inert atmosphere.

Heterocyclic and cluster organoaluminium compounds containing various sequences of Al–N bonds are discussed on p. 265.

Organometallic compounds of Ga, In and Tl

Organometallic compounds of Ga, In and Tl have been less studied than their Al analogues. The trialkyls do not dimerize and there is a general tendency to diminishing thermal stability with increasing atomic weight of M. There is also

a general decrease of chemical reactivity of the M–C bond in the sequence $\text{Al} > \text{Ga} \approx \text{In} > \text{Tl}$, and this is particularly noticeable for compounds of the type R_2MX ; indeed, Tl gives air-stable non-hydrolysing ionic derivatives of the type $[\text{TlR}_2]\text{X}$, where $\text{X} = \text{halogen, CN, NO}_3, \frac{1}{2}\text{SO}_4$, etc. For example, the ion $[\text{TlMe}_2]^+$ is stable in aqueous solution, and is linear like the isoelectronic HgMe_2 and $[\text{PbMe}_2]^{2+}$.

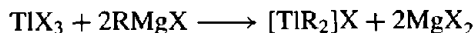
GaR_3 can be prepared by alkylating Ga with HgR_2 or by the action of RMgBr or AlR_3 on GaCl_3 . They are low-melting, mobile, flammable liquids. The corresponding In and Tl compounds are similar but tend to have higher mps and bps; e.g.

Compound	GaMe_3	InMe_3	TlMe_3
MP	–16°	88.4°	38.5°
BP	56°	136°	147° (extrap)
Compound	GaEt_3	InEt_3	TlEt_3
MP	–82°	–	–63°
BP	143°	84°/12 mmHg	192° (extrap)

The triphenyl analogues are also monomeric in solution but tend to associate into chain structures in the crystalline state as a result of weak intermolecular $\text{M} \cdots \text{C}$ interactions: GaPh_3 mp

⁷⁹ V. L. GOEDKEN, H. ITO and T. ITO, *J. Chem. Soc., Chem. Commun.*, 1453–5 (1984).

166°, InPh₃ mp 208°, TlPh₃ mp 170°. For Ga and In compounds the primary M–C bonds can be cleaved by HX, X₂ or MX₃ to give reactive halogen-bridged dimers (R₂MX)₂. This contrasts with the unreactive ionic compounds of Tl mentioned above, which can be prepared by suitable Grignard reactions:



As in the case of organoaluminium compounds, unusual stereochemistries can be imposed by suitable design of ligands. Thus, reaction of GaCl₃ with 3,3',3''-nitriлотris(propylmagnesium chloride), $[\text{N}\{\overline{(\text{CH}_2)_3\text{MgCl}}\}_3]$, yields colourless crystals of $[\text{Ga}(\text{CH}_2)_3\text{N}]$ in which intramolecular N→Ga coordination stabilizes a planar trigonal monopyramidal geometry about Ga and tetrahedral coordination about N, as shown schematically in Fig. 7.20(a).⁽⁸⁰⁾ Because of steric constraints, the Ga–N distance of 209.5 pm is about 7% longer than the sum of the covalent radii (195 pm), although not so long as in Me₃GaNMe₃ (220 pm). Long bonds are also a feature of the unique 6-coordinate complex of InMe₃ with the heterocyclic triazine ligand (PrⁱNCH₂)₃. The air-sensitive adduct, $[\text{Me}_3\text{In}\{\eta^3\text{-(Pr}^i\text{NCH}_2)_3\}]$, can be prepared by

⁸⁰ H. SCHUMANN, U. HARTMANN, A. DIETRICH and J. PICKARDT, *Angew. Chem. Int. Edn. Engl.* **27**, 1077–8 (1988).

direct reaction of the donor and acceptor in ether solution, and is the first example of a tridentate cyclotriazine complex; it is also the first example of InMe₃ accepting three lone pairs of electrons rather than the more usual one or two.⁽⁸¹⁾ The structure (Fig. 7.20b) features a shallow InC₃ pyramid with C–In–C angles of 114°–117° and extremely acute N–In–N angles (48.6°) associated with the long In–N bonds (278 pm). The three Prⁱ groups are all in equatorial positions.

Cyclopentadienyl and arene complexes of Ga, In and Tl have likewise attracted increasing attention during the past decade and provide a rich variety of structural types and of chemical diversity. $[\text{Ga}(\text{C}_5\text{H}_5)_3]$, prepared directly from GaCl₃ and an excess of LiC₅H₅ in Et₂O, was found to have simple trigonal planar Ga bonded to three η¹-C₅H₅ groups. The more elusive C₅Me₅ derivative was finally prepared from GaCl₃ and an excess of the more reactive NaC₅Me₅ in thf solution, or by reduction of Ga(C₅Me₅)_nCl_{3–n} (n = 1, 2) with sodium naphthalene in thf.⁽⁸²⁾ $[\text{Ga}(\text{C}_5\text{Me}_5)_3]$

⁸¹ D. C. BRADLEY, D. M. FRIGO, I. S. HARDING, M. B. HURSTHOUSE and M. MOTEVALLI, *J. Chem. Soc., Chem. Commun.*, 577–8 (1992).

⁸² O. T. BEACHLEY and R. B. HALLOCK, *Organometallics* **6**, 170–2 (1987).

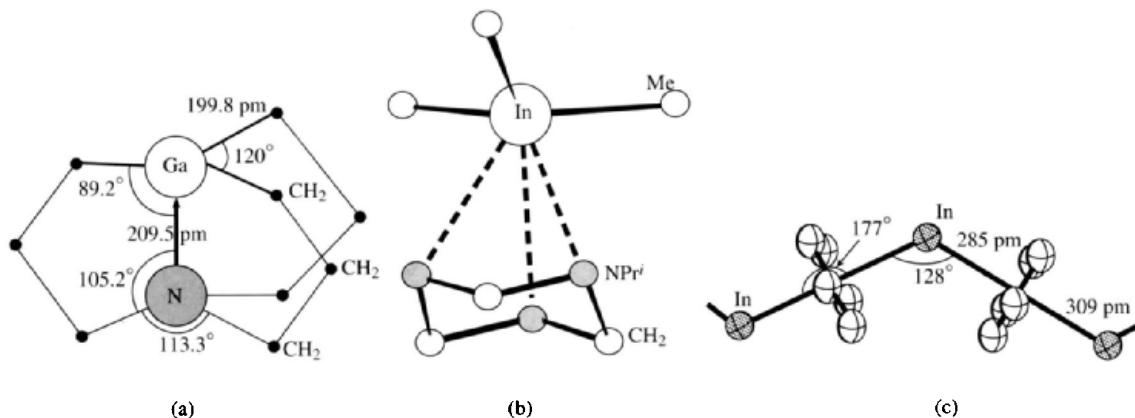


Figure 7.20 (a) Structure of $[\text{Ga}(\text{CH}_2)_3\text{N}]$ showing trigonal planar monopyramidal 4-fold coordination about Ga and tetrahedral coordination about N. (b) Structure of $[\text{Me}_3\text{In}\{\eta^3\text{-(Pr}^i\text{NCH}_2)_3\}]$ — see text for dimensions. (c) Structure of polymeric $[\text{In}(\eta^5\text{-C}_5\text{H}_5)]$.

is a colourless, sublimable, crystalline solid, mp 168°, and appears to be a very weak Lewis acid.

As distinct from the cyclopentadienyls of Ga^{III}, those of In and Tl involve the +1 oxidation state of the metal and pentahapto bonding of the ligand. [In(η^5 -C₅H₅)] is best prepared by metathesis between LiC₅H₅ and a slurry of InCl in Et₂O.⁽⁸³⁾ It is monomeric in the gas phase with a 'half-sandwich' structure, the In–C₅(centroid) distance being 232 pm, but in the solid state it is a zig-zag polymer with significantly larger In–C₅(centroid) distances as shown in Fig. 7.20c.⁽⁸⁴⁾ The crystalline pentamethyl derivative, by contrast, is hexameric and features an octahedral In₆ cluster each vertex of which is η^5 -coordinated by C₅Me₅.⁽⁸⁵⁾ [Tl(η^5 -C₅H₅)] precipitates as air-stable yellow crystals when aqueous TlOH is shaken with cyclopentadiene. In the gas phase the compound is monomeric with C_{5v} symmetry, the Tl atom being 241 pm above the plane of the ring (microwave), whereas in the crystalline phase there are zig-zag chains of equispaced alternating

C₅H₅ rings and Tl atoms similar to the In homologue.

Hexahapto (η^6 -arene) complexes of Ga^I and In^I can be obtained from solutions of the lower halides (p. 240) in aromatic solvents, and some of these have surprisingly complex structures.⁽⁸⁶⁾ With bulky ligands such as C₆Me₆ simple adducts crystallize in which the cations [M(η^6 -C₆Me₆)]⁺ have the C_{6v} 'half-sandwich' structure shown in Fig. 7.21a, e.g. [Ga(η^6 -C₆Me₆)] [GaCl₄] mp 168° and [Ga(η^6 -C₆Me₆)] [GaBr₄] mp 146°.⁽⁸⁷⁾ With less bulky ligands such as mesitylene (1,3,5-C₆H₃Me₃), a 2:1 stoichiometry is possible to give cations [M(η^6 -C₆H₃Me₃)₂]⁺ shown schematically in Fig. 7.21b, although further ligation from the anion may also occur; e.g. [In(η^6 -C₆H₃Me₃)₂] [InBr₄] features polymeric helical chains in which bridging [μ - η^1, η^2 -InBr₄] units connect the cations as shown in Fig. 7.21c.⁽⁸⁸⁾ With still less bulky ligands such as benzene itself, discrete dimers can be formed as in the solvated complex [Ga(η^6 -C₆H₆)₂] [GaCl₄].3C₆H₆. This features tilted bis(arene)Ga^I units linked through bridging GaCl₄ units to form the dimeric structure shown in Fig. 7.22a.⁽⁸⁶⁾ Mixed adducts can also be prepared. Thus, when

⁸³ C. PEPPE, D. G. TUCK and L. VICTORIANO, *J. Chem. Soc., Dalton Trans.*, 2592 (1981).

⁸⁴ O. T. BEACHLEY, J. C. PAZIK, T. E. GLASSMAN, M. R. CHURCHILL, J. C. FETTINGER and R. BLOM, *Organometallics* **7**, 1051–9 (1988).

⁸⁵ O. T. BEACHLEY, M. R. CHURCHILL, J. C. FETTINGER, J. C. PAZIK and L. VICTORIANO, *J. Am. Chem. Soc.* **108**, 4666–8 (1986).

⁸⁶ H. SCHMIDBAUR, *Angew. Chem. Int. Edn. Engl.* **24**, 893–904 (1985).

⁸⁷ H. SCHMIDBAUR, U. THEWALT and T. ZAFIROPOULOS, *Angew. Chem. Int. Edn. Engl.* **23**, 76–7 (1984).

⁸⁸ J. EBENHÖCH, G. MÜLLER, J. RIEDE and H. SCHMIDBAUR, *Angew. Chem. Int. Edn. Engl.* **23**, 386–8 (1984).

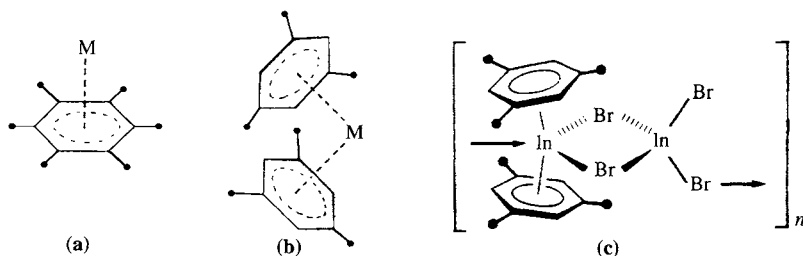


Figure 7.21 (a) The 'half-sandwich' C_{6v} structure characteristic of [Ga(η^6 -C₆Me₆)]⁺. (b) The 'bent-sandwich' structure found in ions of the type [In(η^6 -C₆H₃Me₃)₂]⁺. (c) A section of the helical chain in [In(η^6 -mes)₂][InBr₄] showing the [μ - η^1, η^2 -InBr₄] unit bridging ions of the type shown in (b); the tilting angle is 133° and the ring-centres of the two arene ligands are almost equidistant from In (283 and 289 pm).

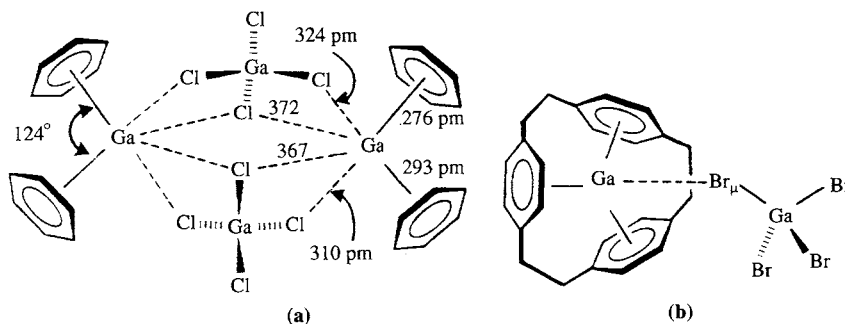


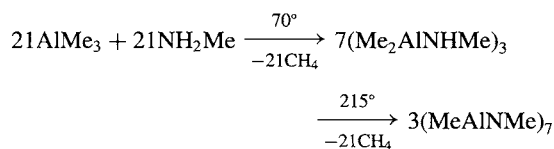
Figure 7.22 (a) Structure of the dimeric unit in the solvated complex $[\text{Ga}(\eta^6\text{-C}_6\text{H}_6)_2][\text{GaCl}_4] \cdot 3\text{C}_6\text{H}_6$ indicating the principal dimensions; the six benzene molecules of solvation per dimer lie outside the coordination spheres of the gallium atoms. (b) Structure of the ion-pair $[\text{Ga}(\eta^{18}\text{-[2.2.2]paracyclophane})][\text{GaBr}_4]$; the four Ga–Br distances within the tetrahedral anion are in the range 230.5–233.3 pm, the distance for Ga–Br $_{\mu}$ being 231.9 pm; the Ga $^1 \cdots$ Br $_{\mu}$ distance is 338.8 pm.

dilute toluene solutions of Ga_2Cl_4 and durene (1,2,4,5- $\text{C}_6\text{H}_2\text{Me}_4$) are cooled to 0° , crystals containing the centrosymmetric dimer $[\{\text{Ga}(\eta^6\text{-dur})(\eta^6\text{-tol})\}\text{GaCl}_4]_2$ are obtained.⁽⁸⁹⁾ The structure resembles that in Fig. 7.22a, with each Ga 1 centre η^6 -bonded to one durene molecule at 264 pm and one toluene molecule at 304 pm. These bent-sandwich moieties are then linked into dimeric units via three of the four Cl atoms of each of the two GaCl_4 tetrahedra.

An even more remarkable structure emerges for the monomeric complex of Ga_2Br_4 with the tris(arene) ligand [2.2.2]paracyclophane (Fig. 7.22b):⁽⁹⁰⁾ the Ga 1 centre is encapsulated in a unique η^{18} environment which has no parallels even in transition-metal coordination chemistry. The Ga $^+$ cation is almost equidistant from the three ring centres (265 pm) but is displaced away from the ligand centre by 43 pm towards the GaBr_4^- counter anion. The complex was prepared by dissolving the dimeric benzene complex $[\{(\text{C}_6\text{H}_6)_2\text{Ga} \cdot \text{GaBr}_4\}_2]$ (cf. Fig. 7.22a) in benzene and adding the cyclophane.

Al–N heterocycles and clusters

Finally, in this chapter, attention should be drawn to a remarkable range of heterocyclic and cluster organoaluminium compounds containing various sequences of Al–N bonds⁽⁹¹⁾ (cf. B–N compounds, p. 207). Thus the adduct $[\text{AlMe}_3(\text{NH}_2\text{Me})]$ decomposes at 70°C with loss of methane to give the cyclic amido trimers *cis*- and *trans*- $[\text{Me}_2\text{AlNHMe}]_3$ (structures 2 and 3) and at 215° to give the oligomeric imido cluster compounds $(\text{MeAlNMe})_7$ (structure 6) and $(\text{MeAlNMe})_8$ (structure 7), e.g.:



Similar reactions lead to other oligomers depending on the size of the R groups and the conditions of the reaction, e.g. *cyclo*- $(\text{Me}_2\text{AlNMe}_2)_2$ (structure 1) and the imido-clusters $(\text{PhAlNPh})_4$, $(\text{HAlNPr}^i)_4$ or 6,

⁸⁹ H. SCHMIDBAUR, R. NOWAK, B. HUBER and G. MÜLLER, *Polyhedron* **9**, 283–7 (1990).

⁹⁰ H. SCHMIDBAUR, R. HAGER, B. HUBER and G. MÜLLER, *Angew. Chem. Int. Edn. Engl.* **26**, 338–40 (1987). See also H. SCHMIDBAUR, W. BUBLAK, B. HUBER and G. MÜLLER, *Organometallics* **5**, 1647–51 (1986).

⁹¹ S. AMIRKHALILI, P. B. HITCHCOCK and J. D. SMITH, *J. Chem. Soc., Dalton Trans.*, 1206–12 (1979); and references 1–9 therein. See also P. P. POWER, *J. Organometallic Chem.* **400**, 49–69 (1990); K. M. WAGGONER, M. M. OLMSTEAD and P. P. POWER, *Polyhedron* **9**, 257–63 (1990); A. J. DOWNS, D. DUCKWORTH, J. C. MACHELL and C. R. PULHAM, *Polyhedron* **11**, 1295–304 (1992).

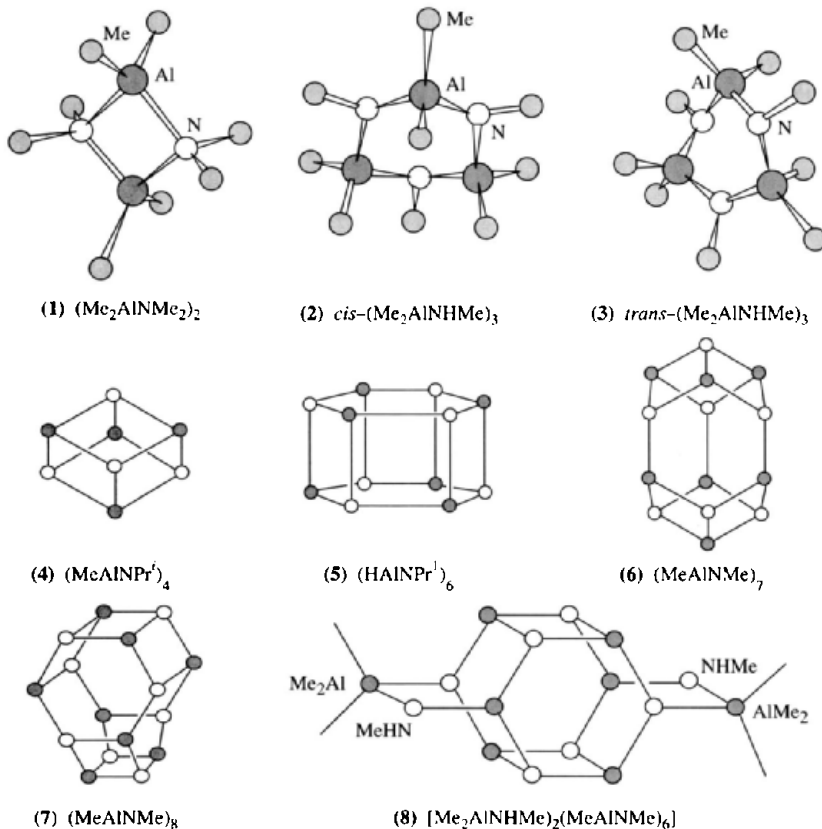
(HAINPrⁿ)₆ or 8, (HAINBu^t)₄, and (MeAlNPr^t)₄ or 6 (see structures 4, 5, 7). Intermediate amido-imido compounds have also been isolated from the reaction, e.g. [Me₂AlNHMe]₂ (MeAlNMe)₆ (structure 8). Oligomers up to (RAINR^t)₁₆ have been obtained although not necessarily structurally characterized. The known structures are all built up from varying numbers of fused 4-membered and 6-membered AlN heterocycles.

Until recently tetramers such as (4) were the smallest oligomers involving alternating Al and N atoms. It will be noted, however, that the hexamer (5) comprises a hexagonal prism formed by conjoining two plane six-membered rings. By increasing the size of the exocyclic groups it has proved possible to isolate a planar trimer, (MeAlNAr)₃, which is isoelectronic with borazine (p. 210). Thus, thermolysis of a mixture of AlMe₃ and ArNH₂

(Ar = 2, 6-Pr^t₂C₆H₃) in toluene at 110° results in the smooth elimination of CH₄ to give the dimer, (Me₂AlNAr)₂, which, when heated to 170°, loses more methane to give a high yield of the trimer, (MeAlNAr)₃, as colourless, air- and moisture-sensitive crystals.⁽⁹²⁾ The six *ipso*-C atoms are coplanar with the planar 6-membered Al₃N₃ ring and the Al-N distance of 178 pm is significantly shorter than in the higher (4-coordinate) oligomers (189–196 pm). Comparison with other 3-coordinate Al and N centres is difficult because of the paucity of examples but the homoleptic monomer [Al{N(SiMe₃)₂}₃] has also been reported to have Al-N distances of 178 pm.

Several analogous gallium compounds are also known, e.g. [(Me₂GaNHMe)₂(MeGaNMe)₆]

⁹² K. M. WAGGONER, H. HOPE and P. P. POWER, *Angew. Chem. Int. Edn. Engl.* **27**, 1699–700 (1988).



(structure 8).⁽⁹¹⁾ Likewise, $(R_2GaPBU'_2)_2$ and $(R_2GaAsBu'_2)_2$ ($R = Me, Bu^t$) have structures analogous to (1).⁽⁹³⁾ A more complex 12-membered Ga_5As_7 cluster has been characterized in $[(PhAsH)(R_2Ga)(PhAs)_6(RGa)_4]$ ($R = Me_3SiCH_2$).⁽⁹⁴⁾ The cyclic trimer, $[\{(triph)GaP(chex)\}_3]$, (where triph = 2,4,6- $Ph_3C_6H_2$ and chex = cyclo- C_6H_{11}) is of interest in being the first well characterized heterocycle consisting entirely of heavier main-group elements. It is obtained as pale yellow crystals by reacting

⁹³ A. M. ARIF, B. L. BENAC, A. H. COWLEY, R. GEERTS, R. A. JONES, K. B. KIDD, J. M. POWER and S. T. SCHWAB, *J. Chem. Soc., Chem. Commun.*, 1543–5 (1986).

⁹⁴ R. L. WELLS, A. P. PURDY, A. T. MCPHAIL and C. G. PITT, *J. Chem. Soc., Chem. Commun.*, 487–8 (1986).

(triph)GaCl₂ with Li₂P(chex) and is formally isoelectronic with borazine (p. 210). Indeed, it has short Ga–P distances (mean 229.7 pm) but the ring is markedly non-planar and there is a slight, statistically significant alternation in Ga–P distances with three averaging at 228.5(4) pm and three at 230.8(4) pm.⁽⁹⁵⁾ Much of the burgeoning interest in this area of volatile compounds of Group 13 elements has come from attempts to devise effective routes to thin films of III–V semiconductors such as GaP, GaAs, etc. via MOCVD (metal-organic chemical vapour deposition).

⁹⁵ H. HOPE, D. C. PESTANA and P. P. POWER, *Angew. Chem. Int. Edn. Engl.* **30**, 691–3 (1991).